Investigational New Drugs (2019) 37:188–198
https://doi.org/10.1007/s10637-018-0682-x

SHORT REPORT

Antitumor evaluation of novel phenothiazine derivatives that inhibit migration and tubulin polymerization against gastric cancer MGC-803 cells

Nan Liu[1] · Zhe Jin[2] · Jing Zhang[2] · Jianjun Jin[2]

Received: 30 August 2018 / Accepted: 23 September 2018 / Published online: 22 October 2018

Summary

Two novel series of 1,2,3-triazole–phenothiazine hybrids and dithiocarbamate–phenothiazine hybrids were designed and synthesized by molecular hybridization strategy. Their antiproliferative activity against three gastric cancer cell lines (MKN28, MGC-803 and MKN45) were evaluated. Among them, hybrid **13h** displayed the most potent inhibitory activity against gastric cancer MGC-803 cells with an IC_{50} value of 1.2 μM. Hybrid **13h** could inhibit migration by regulating the expression level of N-cadherin, E-cadherin, Vimentin, and actived-MMP2. Furthermore, it could regulate wnt/β-catenin signaling pathway on MGC-803 cells in a concentration-dependent manner by decreasing the expression level of Wnt5α, β-catenin and TCF4. From the tubulin polymerization assay results in vitro, hybrid **13h** was a novel tubulin polymerization inhibitor. By oral administration assay, compound **13h** could effectively inhibit MGC-803 xenograft tumor growth in vivo without obvious side effects. In summary, compound **13h** might be an orally active antitumor agent with clinical applications to the treatment of gastric cancer.

Keywords Molecular hybridization strategy · Migration · Tubulin polymerization · Wnt/β-catenin · MGC-803 xenograft tumor growth

Introduction

Microtubules as dynamic polymers of α,β-tubulin displayed important roles in the cell ranging from cell morphology maintenance to subcellular transport, cellular signalling and cell motility [1]. Because of the multiple functions in cancer cells, microtubulin was a highly attractive target for antitumor drugs discovery [2]. Recently, various microtubule-targeting agents were designed [1]. Paclitaxel and its second-generation analogue docetaxel as microtubule-targeting agents were successfully used to treat various cancers in the clinic [3, 4]. However, the limitations of their dose-limiting toxicities and drug resistance prompt the development of novel classes of microtubule-targeting agents [5].

Phenothiazine skeleton was used to design and synthesize novel anticancer agents in medicinal chemistry [6]. Phenothiazine analogue **1** (Fig. 1) exhibited potent cell growth inhibitory avtivity on human colon Duke's type D, colorectal adenocarcinoma COLO 205 cells and human kidney adenocarcinoma A498 cells [7]. Thiazolo[5,4-b]phenothiazine **2** displayed antiproliferative activity against THP-1 human monocytic leukaemia and HL-60 human promyelocytic cell lines [8]. Phenothiazine carrying a sulfonamide moiety **3** as a potent aromatase inhibitor displayed the potent antitumor activity in vitro against T47D cell line by activation of both intrinsic and extrinsic pathways [9].

Molecular hybridization is a novel strategy in drug design based on the combination of different bioactive fragements to produce a new hybrid with improved affinity and efficacy, when compared to the parent drugs [10]. 1,2,3-Triazole as a anticancer fragement was usually used in molecular hybridization strategy to obtain new anticancer hybrids [11]. Quinoline- 1,2,3-triazole hybrid **4** (Fig. 2) demonstrated the significant activity on the C-32 and SNB-

Electronic supplementary material The online version of this article (https://doi.org/10.1007/s10637-018-0682-x) contains supplementary material, which is available to authorized users.

✉ Nan Liu
zdu581121@163.com

[1] Department of pharmacy, The First Affiliated Hospital of Zhengzhou University, Zhengzhou 450000, China

[2] First Affiliated Hospital of Henan University of Science and Technology, Luoyang 471000, China

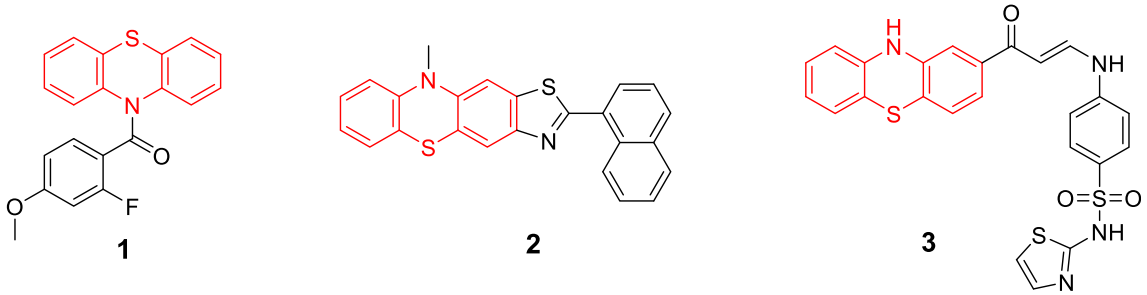

Fig. 1 Phenothiazine derivatives as potent anticancer agents

19 cell lines [12]. Pyrazolo[3,4-d]pyrimidin-4(5*H*)-one tethered to 1,2,3-triazole **5** arrested cell cycle at S phase and induced apoptosis in U87 GBM cell lines [13]. Theophylline containing 1,2,3-triazole **6** displayed potent anticancer activity by targeting human epidermal growth factor receptor 2 [14]. In addition, dithiocarbamate was also used to design anticancer hybrids by molecular hybridization strategy. Dithiocarbamate-nitrostyrene hybrid **7** could inhibit the cancer cell proliferation by inducing apoptosis through caspase-3 activation [15]. Quinoline-dithiocarbamate hybrid **8** exhibited potent anticancer activities on human non-small cell lung cancer cell line H460 [16]. Quinazolin-4(3*H*)-one-dithiocarbamate hybrid **9** inhibited proliferation of A549, MCF-7, HeLa, HT29 and HCT-116 cells with IC_{50} values of 5.44, 7.15, 12.16, 10.35 and 11.44 μM, respectively [17].

In this work, we designed and synthesized novel phenothiazine hybrids bearing 1,2,3-triazole unit and dithiocarbamate unit as tubulin polymerization inhibitors by molecular hybridization strategy. In addition, these phenothiazines were evluated their anticancer mechanisms against gastric cancer MGC-803 cells.

Experimental

Chemistry

Chemical reagents and solvents were purchased from Beijing Yinuokai company. NMR spectra were obtained by a Bruker DPX 600 MHz spectrometer from Shnaghai. For 1,2,3-triazole-phenothiazines, mass spectrawere recorded on Esquire 3000 mass spectrometer by electrospray ionization (ESI).

General synthesis of compounds 13a-13i

10*H*-phenothiazine (3 mmol), acetone (15 mL), propargyl bromide (3 mmol) and NaOH (3 mmol) were added carefully and the reaction mixture was stirred at room temperature for 5 h. Upon completion, the reaction mixture was concentrated under vacuum to afford crude intermediate **12**, which were used in the next reaction without further purification. Crude intermediate **12** (1 mmol), azides (1 mmol), $CuSO_4.5H_2O$ (0.3 mmol) and $Na_2HPO_4.12H_2O$ (0.15 mmol) were dissolved in acetone/H_2O (10 ml/10 ml) to stir for 7 h at room

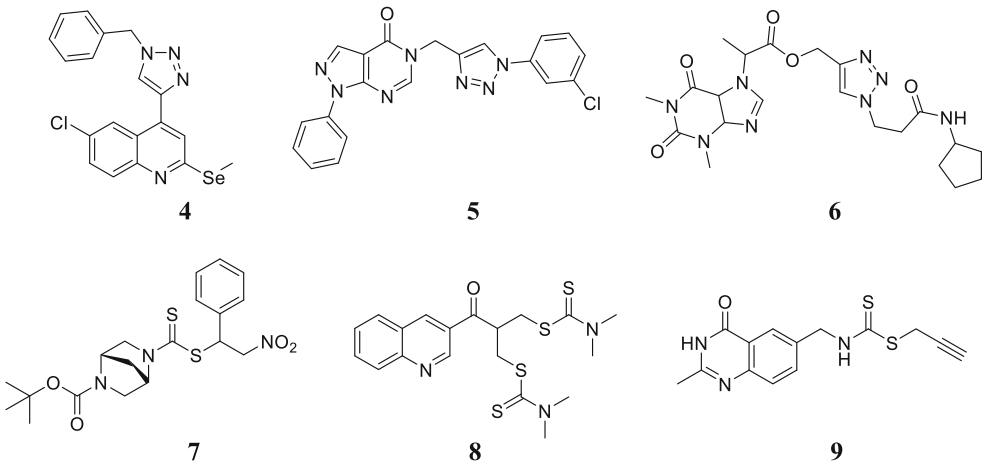

Fig. 2 Anticancer 1,2,3-triazole unit and dithiocarbamate unit used in molecular hybridization strategy

temperature. Upon completion, the crude products were purified with column chromatography on silica gel (hexane/EtOAc = 9/1).

10*H*-phenothiazine (4 mmol), acyl chloride derivatives (4 mmol), acetone (10 ml) and $NaHCO_3$ (5 mmol) were added carefully and the reaction mixture was stirred at room temperature for 3 h. Crude intermediates **14a**~**14d** were obtained by recrystallization. **14a**~**14d** (2 mmol), carbon disulfide (2 mmol), piperazine derivatives (3 mmol) and Et_3N (3 mmol) were dissolved in acetone (7 ml) to stir for 4 h at room temperature. Upon completion, the crude products were purified with column chromatography on silica gel (hexane/EtOAc = 11/1) to obtain **15a**~**15d**.

10-((1-(2-Methoxyphenyl)-1H-1,2,3-triazol-4-yl)methyl)-4a,10a-dihydro-10H-phenothiazine (13a)

Yield:73%, white solid, m.p:171~172 °C. ^{1}H NMR (400 MHz, DMSO-d_6) δ 8.32 (s, 1H), 7.62 (dd, J = 7.9, 1.6 Hz, 1H), 7.55–7.45 (m, 1H), 7.28 (d, J = 7.7 Hz, 1H), 7.20–7.04 (m, 7H), 6.95 (td, J = 7.6, 1.0 Hz, 2H), 5.24 (s, 2H), 3.78 (s, 3H). ^{13}C NMR (100 MHz, DMSO-d_6) δ 151.25, 144.19, 143.22, 130.54, 127.45, 126.79, 125.61, 125.47, 125.28, 122.94, 122.68, 120.89, 115.94, 113.08, 56.07, 43.54. HR-MS (ESI) calcd for $C_{22}H_{21}N_4OS$ $[M+H]^+$: 389.1436, found: 389.1439.

10-((1-(2,4-Dimethoxyphenyl)-1H-1,2,3-triazol-4-yl)methyl)-10H-phenothiazine (13b)

Yield:77%, yellow solid, m.p:157~158 °C. ^{1}H NMR (400 MHz, $CDCl_3$) δ 7.66 (s, 1H), 7.51 (d, J = 8.7 Hz, 1H), 7.12–6.90 (m, 4H), 6.91–6.65 (m, 4H), 6.59–6.35 (m, 2H), 5.21 (s, 2H), 3.75 (s, 3H), 3.60 (s, 3H). ^{13}C NMR (100 MHz, $CDCl_3$) δ 161.26, 152.52, 144.36, 143.80, 127.34, 127.12, 126.32, 124.98, 123.90, 122.79, 119.88, 115.47, 104.72, 99.51, 55.85, 55.69, 45.18. HR-MS (ESI) calcd for $C_{23}H_{23}N_4O_2S$ $[M+H]^+$: 419.1542, found: 419.1548.

10-((1-(3,5-Dimethoxyphenyl)-1H-1,2,3-triazol-4-yl)methyl)-4a,10a-dihydro-10H-phenothiazine(13c)

Yield:83%, yellow solid, m.p:140~142 °C. ^{1}H NMR (400 MHz, DMSO-d_6) δ 8.33 (s, 1H), 7.24 (d, J = 3.1 Hz, 1H), 7.21 (d, J = 9.2 Hz, 1H), 7.16 (ddd, J = 7.5, 6.2, 1.4 Hz, 4H), 7.11–7.04 (m, 3H), 6.95 (td, J = 7.5, 1.0 Hz, 2H), 5.24 (s, 2H), 3.76 (s, 3H), 3.72 (s, 3H). ^{13}C NMR (100 MHz, DMSO-d_6) δ 153.18, 145.02, 144.19, 143.28, 127.46, 126.80, 125.89, 125.41, 122.95, 122.69, 115.95, 115.61, 114.48, 110.46, 56.55, 55.76, 43.47. HR-MS (ESI) calcd for $C_{23}H_{23}N_4O_2S$ $[M+H]^+$: 419.1542, found: 419.1546.

10-((1-(3,4-Dimethoxyphenyl)-1H-1,2,3-triazol-4-yl)methyl)-4a,10a-dihydro-10H-phenothiazine (13d)

Yield:86%, yellow solid, m.p:201~202 °C. ^{1}H NMR (400 MHz, DMSO-d_6) δ 8.60 (s, 1H), 7.37 (d, J = 2.5 Hz, 1H), 7.31 (dd, J = 8.7, 2.5 Hz, 1H), 7.11–7.04 (m, 4H), 7.01 (d, J = 8.8 Hz, 1H), 6.94 (dd, J = 5.9, 2.8 Hz, 2H), 6.86 (td, J = 7.5, 1.0 Hz, 2H), 5.14 (s, 2H), 3.76 (s, 3H), 3.73 (s, 3H). ^{13}C NMR (100 MHz, DMSO-d_6) δ 149.30, 148.83, 144.35, 144.10, 129.98, 127.51, 126.73, 122.69, 122.65, 121.54, 115.76, 111.99, 104.50, 55.87, 55.79, 43.85. HR-MS (ESI) calcd for $C_{23}H_{23}N_4O_2S$ $[M+H]^+$: 419.1542, found: 419.1549.

(3-(4-((4,10-Dihydro-10H-phenothiazin-10-yl)methyl)-1H-1,2,3-triazol-1-yl)phenyl)methanol(13e)

Yield:68%, yellow solid, m.p:186~188 °C. ^{1}H NMR (400 MHz, DMSO-d_6) δ 8.69 (s, 1H), 7.84 (s, 1H), 7.74 (d, J = 7.9 Hz, 1H), 7.51 (t, J = 7.8 Hz, 1H), 7.41 (d, J = 7.6 Hz, 1H), 7.14 (t, J = 7.0 Hz, 4H), 7.02 (d, J = 8.0 Hz, 2H), 6.93 (t, J = 7.4 Hz, 2H), 5.38 (t, J = 5.7 Hz, 1H), 5.23 (s, 2H), 4.59 (d, J = 5.7 Hz, 2H). ^{13}C NMR (100 MHz, DMSO-d_6) δ 144.77, 144.59, 144.05, 136.40, 129.54, 127.52, 126.73, 126.35, 122.65, 122.64, 121.51, 118.11, 117.68, 115.73, 62.27, 43.81. HR-MS (ESI) calcd for $C_{22}H_{21}N_4OS$ $[M+H]^+$: 389.1436, found: 389.1438.

1-(4-(4-((4,10-Dihydro-10H-phenothiazin-10-yl)methyl)-1H-1,2,3-triazol-1-yl)phenyl)ethan-1-one (13f)

Yield:65%, white solid, m.p:185~186 °C. ^{1}H NMR (400 MHz, DMSO-d_6) δ 8.80 (s, 1H), 8.06 (d, J = 8.8 Hz, 2H), 8.00 (d, J = 8.8 Hz, 2H), 7.07 (t, J = 7.4 Hz, 4H), 6.94 (d, J = 7.8 Hz, 2H), 6.87 (t, J = 7.4 Hz, 2H), 5.18 (s, 2H), 2.55 (s, 3H). ^{13}C NMR (100 MHz, DMSO-d_6) δ 145.01, 144.02, 139.45, 130.00, 127.54, 126.74, 122.69, 121.76, 119.65, 115.74, 112.43, 43.75, 26.78. HR-MS (ESI) calcd for $C_{23}H_{21}N_4OS$ $[M+H]^+$: 401.1436, found: 401.1438.

10-((1-(3-Nitrophenyl)-1H-1,2,3-triazol-4-yl)methyl)-4a,10a-dihydro-10H-phenothiazine(13g)

Yield:91%, white solid, m.p:149~150 °C. ^{1}H NMR (400 MHz, DMSO-d_6) δ 8.80 (s, 1H), 8.06 (d, J = 8.8 Hz, 2H), 8.00 (d, J = 8.8 Hz, 2H), 7.07 (t, J = 7.4 Hz, 4H), 6.94 (d, J = 7.8 Hz, 2H), 6.87 (t, J = 7.4 Hz, 2H), 5.18 (s, 2H), 2.55 (s, 3H). ^{13}C NMR (100 MHz, DMSO-d_6) δ 145.01, 144.02, 139.45, 130.00, 127.54, 126.74, 122.69, 121.76, 119.65, 115.74, 112.43, 43.75, 26.78. HR-MS (ESI) calcd for $C_{21}H_{18}N_5O_2S$ $[M+H]^+$: 404.1181, found: 404.1189.

10-((1-(4-Methoxy-2-nitrophenyl)-1H-1,2,3-triazol-4-yl) methyl)-4a,10a-dihydro-10H-phenothiazine (13h)

Yield:72%, white solid, m.p:149~150 °C. ^{1}H NMR (400 MHz, DMSO-d_6) δ 8.51 (s, 1H), 8.03 (s, 1H), 8.00 (s, 2H), 7.17 (dd, J = 10.9, 4.3 Hz, 4H), 7.06 (d, J = 8.0 Hz, 2H), 6.95 (t, J = 7.4 Hz, 2H), 5.27 (s, 2H), 3.95 (s, 3H). ^{13}C NMR (100 MHz, DMSO-d_6) δ 151.18, 148.00, 144.13, 143.80, 130.43, 127.46, 126.82, 125.55, 125.53, 123.01, 122.74, 116.25, 115.95, 108.38, 57.04, 43.38. HR-MS (ESI) calcd for $C_{22}H_{20}N_5O_3S$ $[M+H]^+$: 434.1287, found: 434.1289.

10-((1-(2-Methoxy-4-nitrophenyl)-1H-1,2,3-triazol-4-yl) methyl)-4a,10a-dihydro-10H-phenothiazine (13i)

Yield:72%, white solid, m.p:191~192 °C. ^{1}H NMR (400 MHz, DMSO-d_6) δ 8.54 (s, 1H), 8.03 (s, 1H), 7.70 (dt, J = 19.2, 4.6 Hz, 2H), 7.14 (ddd, J = 6.4, 4.0, 1.5 Hz, 4H), 7.06–6.86 (m, 4H), 5.25 (s, 2H), 2.48 (s, 3H). ^{13}C NMR (100 MHz, DMSO-d_6) δ 144.21, 143.98, 143.72, 141.78, 134.54, 127.49, 127.31, 126.71, 125.44, 124.93, 122.68, 122.57, 115.73, 43.85, 20.36. HR-MS (ESI) calcd for $C_{22}H_{20}N_5O_3S$ $[M+H]^+$: 434.1287, found: 434.1288.

2-Chloro-1-(10H-phenothiazin-10-yl)ethan-1-one (14a)

Light yellow solid, yield:61%, mp:120–122 °C. ^{1}H NMR (400 MHz, DMSO-d_6) δ 7.70 (d, J = 7.8 Hz, 2H), 7.60 (dd, J = 7.7, 1.1 Hz, 2H), 7.43 (td, J = 7.7, 1.4 Hz, 2H), 7.35 (td, J = 7.6, 1.1 Hz, 2H), 4.51 (s, 2H). ^{13}C NMR (100 MHz, DMSO-d_6) δ 171.16, 165.47, 138.07, 132.75, 128.55, 128.47, 127.98, 127.85, 127.71, 127.56, 127.39, 43.22. HR-MS (ESI) calcd for $C_{14}H_{11}ClNOS$ $[M+H]^+$: 276.0250, found: 276.0256.

3-Chloro-1-(10H-phenothiazin-10-yl)propan-1-one (14b)

Green solid, yield:26%, mp:140-143 °C. ^{1}H NMR (400 MHz, DMSO-d_6) δ 7.64 (d, J = 7.9 Hz, 2H), 7.58 (d, J = 7.8 Hz, 2H), 7.42 (t, J = 7.6 Hz, 2H), 7.33 (t, J = 7.6 Hz, 2H), 3.63 (t, J = 6.3 Hz, 2H), 2.51 (d, J = 1.3 Hz, 2H). ^{13}C NMR (100 MHz, DMSO-d_6) δ 168.86, 138.46, 128.47, 127.86, 127.79, 127.67, 37.46, 28.80. HR-MS (ESI) calcd for $C_{15}H_{13}ClNOS$ $[M+H]^+$: 290.0406, found: 290.0409.

4-Chloro-1-(10H-phenothiazin-10-yl)butan-1-one (14c)

Gray green solid, yield:53%, mp:95-99 °C. ^{1}H NMR (400 MHz, DMSO-d_6) δ 7.64 (d, J = 7.4 Hz, 2H), 7.57 (dd, J = 7.7, 1.2 Hz, 2H), 7.41 (td, J = 7.7, 1.4 Hz, 2H), 7.32 (td, J = 7.6, 1.2 Hz, 2H), 3.58 (t, J = 6.5 Hz, 2H), 2.60 (s, 2H), 1.93 (p, J = 6.8 Hz, 2H). ^{13}C NMR (100 MHz, DMSO-d_6) δ 170.77, 138.83, 132.80, 128.43, 128.03, 127.78, 127.55, 45.07, 31.37, 28.23. HR-MS (ESI) calcd for $C_{16}H_{15}ClNOS$ $[M+H]^+$: 304.0563, found: 304.0567.

5-Chloro-1-(10H-phenothiazin-10-yl)pentan-1-one (14d)

White solid, yield:67%, mp:99-103 °C. ^{1}H NMR (400 MHz, $CDCl_3$) δ 7.42 (d, J = 7.8 Hz, 2H), 7.37 (dd, J = 7.7, 1.1 Hz, 2H), 7.30–7.21 (m, 2H), 7.21–7.11 (m, 2H), 3.37 (t, J = 6.1 Hz, 2H), 2.42 (s, 2H), 1.79–1.55 (m, 4H). ^{13}C NMR (100 MHz, $CDCl_3$) δ 170.57, 137.73, 132.29, 127.02, 126.24, 125.99, 125.87, 43.56, 32.35, 30.69, 21.55. HR-MS (ESI) calcd for $C_{17}H_{17}ClNOS$ $[M+H]^+$: 318.0719, found: 318.0723.

2-Oxo-2-(10H-phenothiazin-10-yl)ethyl-4-(pyridin-2-yl)piperazine-1-carbodithioate (15a) Light yellow solid, yield:6%, mp:185-188 °C. ^{1}H NMR (400 MHz, DMSO-d_6) δ 8.12 (dd, J = 4.9, 1.3 Hz, 1H), 7.70 (d, J = 7.1 Hz, 2H), 7.63–7.50 (m, 3H), 7.42 (td, J = 7.8, 1.2 Hz, 2H), 7.33 (t, J = 7.2 Hz, 2H), 6.79 (d, J = 8.6 Hz, 1H), 6.67 (dd, J = 6.8, 5.0 Hz, 1H), 4.44 (s, 2H), 4.22 (s, 2H), 4.01 (s, 2H), 3.62 (s, 4H). ^{13}C NMR (100 MHz, DMSO-d_6) δ 194.60, 166.26, 158.60, 148.04, 138.45, 138.16, 128.40, 127.84,127.66, 113.79, 107.45, 44.06. HR-MS (ESI) calcd for $C_{24}H_{23}N_4OS_3$ $[M+H]^+$: 479.1034, found: 479.1039.

3-Oxo-3-(10H-phenothiazin-10-yl)propyl 4-(pyridin-2-yl)piperazine-1-carbodithioate (15b) White solid, yield:80%, mp:114-117 °C. ^{1}H NMR (400 MHz, DMSO-d_6) δ 8.13 (d, J = 3.4 Hz, 1H), 7.71–7.47 (m, 5H), 7.41 (dd, J = 10.9, 4.3 Hz, 2H), 7.31 (t, J = 7.5 Hz, 2H), 6.80 (d, J = 8.6 Hz, 1H), 6.68 (dd, J = 6.8, 5.1 Hz, 1H), 4.28 (s, 2H), 3.96 (s, 2H), 3.63 (s, 4H), 3.48 (t, J = 6.5 Hz, 2H), 2.91 (s, 2H). ^{13}C NMR (100 MHz, DMSO-d_6) δ 194.91, 169.60, 158.13, 147.55, 138.12, 137.63, 127.89, 127.44, 127.28,127.09, 113.25, 106.91, 43.53, 33.48, 31.65. HR-MS (ESI) calcd for $C_{25}H_{25}N_4OS_3$ $[M+H]^+$: 493.1190, found: 493.1197.

3-Oxo-3-(10H-phenothiazin-10-yl)propyl-4-(2-hydroxyethyl)piperazine-1-carbodithioate (15c) Yellow solid, yield:14%, mp:162–164 °C. ^{1}H NMR (400 MHz, DMSO-d_6) δ 7.61 (d, J = 7.8 Hz, 2H), 7.56 (d, J = 7.6 Hz, 2H), 7.40 (t, J = 7.4 Hz, 2H), 7.32 (t, J = 7.4 Hz, 2H), 4.45 (t, J = 5.2 Hz, 1H), 4.16 (s, 2H), 3.82 (s, 2H), 3.51 (dd, J = 11.3, 5.6 Hz, 2H), 3.44 (t, J = 6.3 Hz, 2H), 2.89 (s, 2H), 2.47 (s, 4H), 2.42 (t, J = 6.0 Hz, 2H). ^{13}C NMR (100 MHz, DMSO-d_6) δ 162.12, 156.89, 156.20, 143.80, 138.11, 131.93, 130.36, 130.09, 128.71, 123.70, 123.42, 122.75, 118.77, 117.99,

117.91,114.23, 55.60, 52.26, 38.08. HR-MS (ESI) calcd for $C_{22}H_{26}N_3O_2S_3$ $[M+H]^+$: 460.1187, found: 460.1189.

5-Oxo-5-(10H-phenothiazin-10-yl)pentyl-4-(2-hydroxyethyl)piperazine-1-carbodithioate (15d) Orange liquid, yield:79%. ^{1}H NMR (400 MHz, $CDCl_3$) δ 7.43 (d, J = 7.8 Hz, 2H), 7.37 (dd, J = 7.7, 1.2 Hz, 2H), 7.29–7.22 (m, 2H), 7.16 (td, J = 7.6, 1.2 Hz, 2H), 4.26 (s, 2H), 3.88 (s, 2H), 3.68–3.41 (m, 2H), 3.16 (t, J = 7.0 Hz, 2H), 2.55–2.47 (m, 6H), 2.44 (t, J = 6.7 Hz, 2H), 1.71–1.55 (m, 4H). ^{13}C NMR (100 MHz, $CDCl_3$) δ 196.39, 170.77, 137.74, 132.25, 127.00, 126.29, 125.98, 125.83, 58.12, 56.78, 51.29, 35.65, 32.79, 28.25, 27.06, 23.30. HR-MS (ESI) calcd for $C_{24}H_{30}N_3O_2S_3$ $[M+H]^+$: 488.1500, found: 488.1507.

Biology

MTT assay

Human gastric cancer cells were cultured by RPMI 1640 medium with 10% FBS and 100 U/ml penicillin and 0.1 mg/ml streptomycin in the 37 °C in an atmosphere containing 5% CO_2. MTT assay was used to examine the antiproliferative activity of 1,2,3-triazole-phenothiazines following the reported paper [18].

Migration assay

24-Well cell migration assay was used in the migration by reported papers [19, 20]. MGC-803 cells were treated with hybrid **13h** at different concentrations for 24 h. Then, 10,000 cells were added in each well in 24-Well cell migration plate and cultured for 24 h. Data are presented as mean ± SD from three independent experiments.

Western blot analysis

MGC-803 cells were treated with compound **13h** at different concentrations for 48 h, the cells were collected and lysed. The total protein extracts were boiled with 5 × loading buffer, separated and transferred by PVDF membrane. The membranes were blocked with 5% milk at room temperature for 1 h, and then incubated overnight at 4 °C with primary antibodies. After washing the membrane with the secondary antibody (1:2000) at room temperature for 2 h.

Tubulin polymerization assay in vitro

MGC-803 cells were treated with compound **13h** for 6 h and lysed to do tubulin polymerization assay in vitro by previous method [21]. The buffer was the mixture of 20 mM Tris-HCl, 1 mM PMSF, 1 mM $MgCl_2$, 1 mM orthovanadate, 2 mM EGTA, 0.5% NP-40, and protease inhibitor (pH 6.8). The experimental results were repeated three times.

Animal studies

Animals were obtained from First Affiliated Hospital of Henan University of Science and Technology and these experiments were carried out in accordance with the approved guidelines and approved by the ethics committee. MGC-803 xenograft models were established based on reported papers [22, 23]. Mice were divided into control groups and treatment groups (1,2,3-triazole-phenothiazine hybrid **13h**, 50 mg/kg). The treatment groups received intragastric administration to do in vivo assay.

Results and discussion

Chemistry

Azides were obtained by classical diazotation−azidation reaction from the reported papers [24, 25]. The structures of azides **10a**~**10i** used in this work were listed in Fig. 3.

In order to synthesize phenothiazine-1,2,3-triazole hybrids, 10*H*-phenothiazine **11** was used as starting material. 10*H*-phenothiazine **11** reacted with propargyl bromide at the alkaline condition to form intermediate **12**. Without any purification, the crude system reacted with azides **10a**~**10i** in the presence of disodium phosphate dodecahydrate by copper-catalyzed azide-alkyne cycloaddition reaction to synthesize hybrids **13a**~**13i** (Scheme 1).

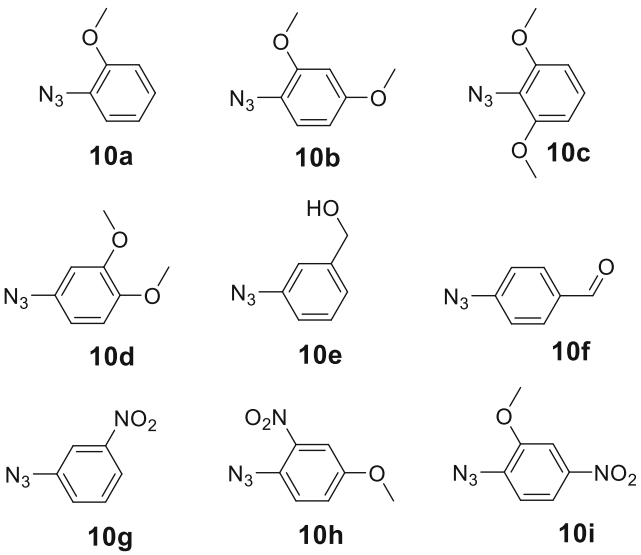

Fig. 3 The structures of azides **10a**~**10i** used in this work

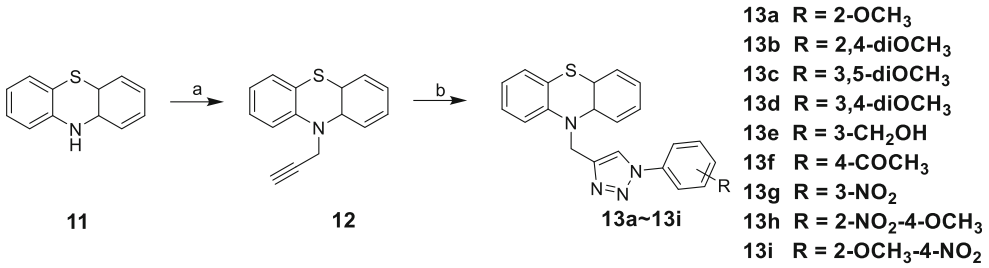

Scheme 1 Synthesis of 1,2,3-triazole–phenothiazine hybrids. Regents and conditions: **a** NaOH, acetone, propargyl bromide, room temperature; **b** $Na_2HPO_4.12H_2O$, $CuSO_4.5H_2O$, azides **13a**~**13i**, acetone/H_2O, room temperature

To synthesize phenothiazine-dithiocarbamate hybrids, 10*H*-phenothiazine **11** reacted with acyl chloride derivatives in the precence of sodium bicarbonate to form intermediate **14a**~**14d**. Piperazine derivatives, carbon disulfide and intermediate **14a**~**14d** were stirred to obtaoin compounds **15a**~**15d** (Scheme 2) in the precence of triethylamine.

Antiproliferative activity evaluation

Gastric cancer as one of the leading causes of death in the world is a heavy burden to public health [26–30]. Many 1,2,3-triazoles displayed the potent anticancer activity against gastric cancer cells [31]. Thus, all 1,2,3-triazole–phenothiazine hybrids were evaluated their anticancer activity in vitro against three gastric cancer cell lines (MKN28, MGC-803 and MKN45) in this work. In the previous papers, 5-fluorouracil was used as a reference drug to compare the antiproliferative activity with 1,2,3-triazoles [32, 33]. So, we also used 5-fluorouracil as a control drug in the antiproliferative activity evaluation.

The anticancer activity results in vitro was listed in Table 1. Compound **11** and compound **12** displayed weak antiproliferative activity with IC_{50} values >100 μM. However, compounds **13a**~**13i** exhibited potent antiproliferative activity with IC_{50} values from 1.2 μM to 20.2 μM. These results revealed that 1,2,3-triazole played the pivotal effect for anticancer activity in vitro.

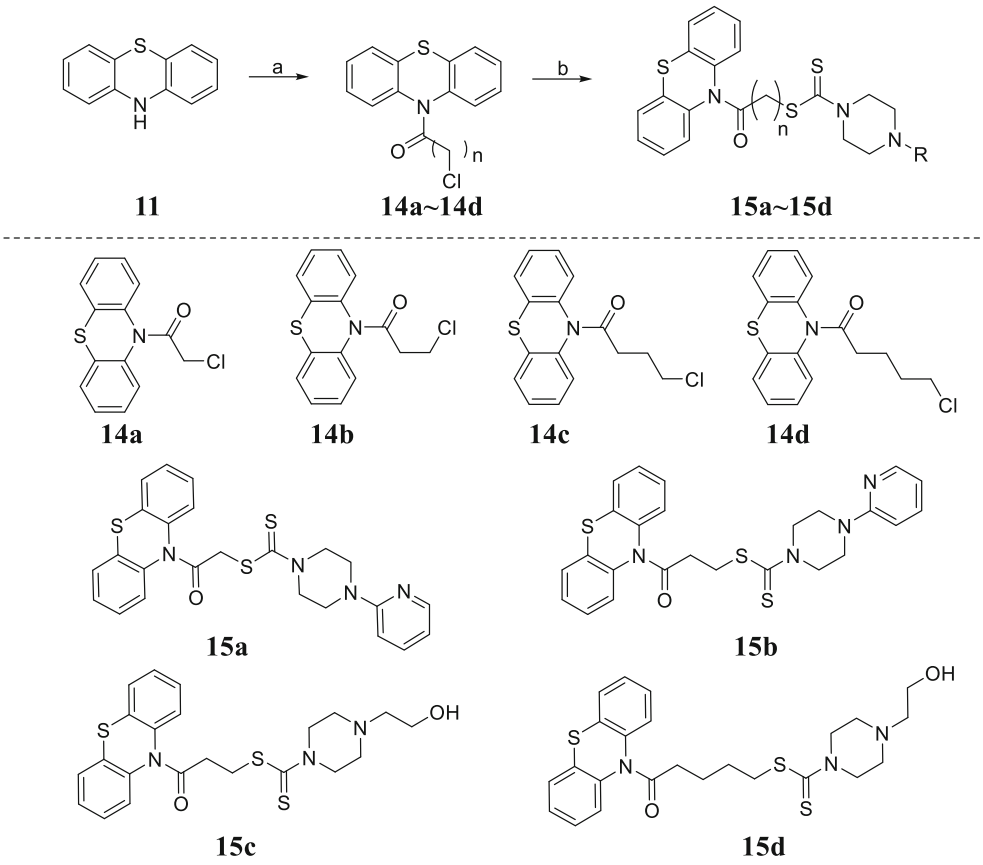

Scheme 2 Synthesis of phenothiazine-dithiocarbamate. Regents and conditions: **a** $NaHCO_3$, acetone, acyl chloride, room temperature; **b** Et_3N, $CuSO_4.5H_2O$, piperazine derivatives, acetone, room temperature

Table 1 Antiproliferative activity of phenothiazine hybrids **13a**~**13i**

Compound	IC_{50} (μM)[a]		
	MKN28	MGC-803	MKN45
11	>100	>100	>100
12	>100	>100	>100
13a	17.5 ± 0.6	20.1 ± 0.9	16.8 ± 1.2
13b	8.3 ± 0.6	12.4 ± 1.0	20.2 ± 1.7
13c	9.2 ± 1.4	17.0 ± 0.6	12.0 ± 1.5
13d	11.3 ± 0.5	13.7 ± 1.1	9.8 ± 0.6
13e	7.6 ± 0.8	12.3 ± 1.2	14.2 ± 0.7
13f	3.5 ± 0.3	8.6 ± 0.9	9.2 ± 1.3
13g	4.5 ± 0.5	7.2 ± 1.7	8.2 ± 1.6
13h	2.7 ± 0.4	1.2 ± 0.1	3.5 ± 0.3
13i	5.3 ± 0.2	4.1 ± 1.3	6.4 ± 1.2
14a	>100	>100	>100
14b	>100	>100	>100
15a	16.5 ± 1.6	17.2 ± 0.8	17.2 ± 0.3
15b	23.1 ± 3.4	18.3 ± 2.4	25.7 ± 3.2
15c	8.7 ± 0.6	10.2 ± 1.6	9.0 ± 1.5
15d	28.0 ± 2.4	24.2 ± 2.3	17.4 ± 1.8
5-Fluorouracil	6.9 ± 0.7	9.4 ± 1.6	19.4 ± 1.4

[a] Antiproliferative activity was assayed by exposure for 48 h. The data are presented as the means of three independent experiments

To explore the structure activity relationship, various 1,2,3-triazole−phenothiazine hybrids with different substituent groups on phenothiazine ring were synthesized. Replacement of the 2,6-diOCH_3 unit on the phenyl ring (**13c**) with a 2-OCH_3 unit (**13a**) led to an decrease in activity, but changing to a 2-OCH_3–4-NO_2 group (**13i**) led to a significant increase in activity against all of the tested cell lines. Importantly, 1,2,3-triazole-phenothiazine hybrid **13h** containing a 2-NO_2–4-OCH_3 group on the phenyl ring exhibited the best antiproliferative activity with an IC_{50} value of 1.2 μM against MGC-803 cells among all hybrids. These results indicated that the substituents on the phenyl ring attaching 1,2,3-triazole skeleton may play a significant role in their inhibitory activity.

For the phenothiazine-dithiocarbamate hybrids **15a**~**15d**, all the hybrids exhibited moderate to potent antiproliferative activity with IC_{50} values from 8.7 μM to 28.0 μM. However, phenothiazine derivatives **14a**~**14b** without dithiocarbamate fragement displayed too weak antiproliferative activity with IC_{50} value >100 μM. These results revealed that dithiocarbamate unit played the important role for anticancer activity of phenothiazine-dithiocarbamate hybrids in vitro. This finding might be useful to design more powerful anticancer drugs in the future.

Compound **13h** was further examined for possible cytotoxicity against GES-1 (normal human gastric epithelial cell line). We found that compound **13h** exhibited no cytotoxicity against GES-1 (>40 μM). The results indicated that compound **13h** had good selectivity between the selected cancer cell line (MGC-803) and a normal cell line (GES-1).

Phenothiazine hybrids inhibited cell proliferation against MGC-803 cells

To investigate antiproliferation ability, MGC-803 cells were added and treated by different 1,2,3-triazole−phenothiazine hybrids in the 24-well plates. From the Fig. 4, 1,2,3-triazole−phenothiazine hybrids exhibited moderate to good anti-proliferation ability against MGC-803 cells. Notably, compounds **13b**, **13e**, **13f**, **13g**, **13h** and **13i** displayed cell proliferation efficiency of 72%, 72%, 52%, 49%, 2 and 17% respectively at 4 μM concentration for 72 h. Among them, compound **13h** showed the most potent antiproliferation efficiency with percentages of 49 and 23% for 48 h and 72 h at 1 μM concentration.

Compound 13h inhibited the migration against MGC-803 cells

From the antiproliferative activity results, we selected the phenothiazine hybrid **13h** to do antiproliferative mechanisms. The effect of migration on MGC-803 cell line with compound **13h** treatment was explored by previous paper using a 24-well migration plate [34]. With the treatment of phenothiazine hybrid **13h** at 2 μM and 4 μM (Fig. 5), the migration rate was decreased to 26 and 4%, respectively. These results showed that phenothiazine hybrid **13h** inhibited the migration of MGC-803 cell line in a concentration-dependent manner.

Compound 10h regulated the epithelial-mesenchymal transition process

Epithelial-mesenchymal transition (EMT) described the molecular reprogramming and phenotypic changes involved in the conversion of polarised immotile epithelial cells to motile mesenchymal cells [35]. E-cadherin and N-cadherin were calcium-dependent cell adhesion molecules, and the loss of E-cadherin–mediated adhesion played a key role in the transition of epithelial tumors [36].

Based on the migration results, we tested the epithelial-mesenchymal transition related markers (N-cadherin, E-cadherin, Vimentin, and actived-MMP2). As the results shown in Fig. 6, phenothiazine hybrid **13h** could upregulate the expression level of E-cadherin and downregulate the expression level of N-cadherin, vimentin and actived-MMP2. These results revealed that phenothiazine hybrid

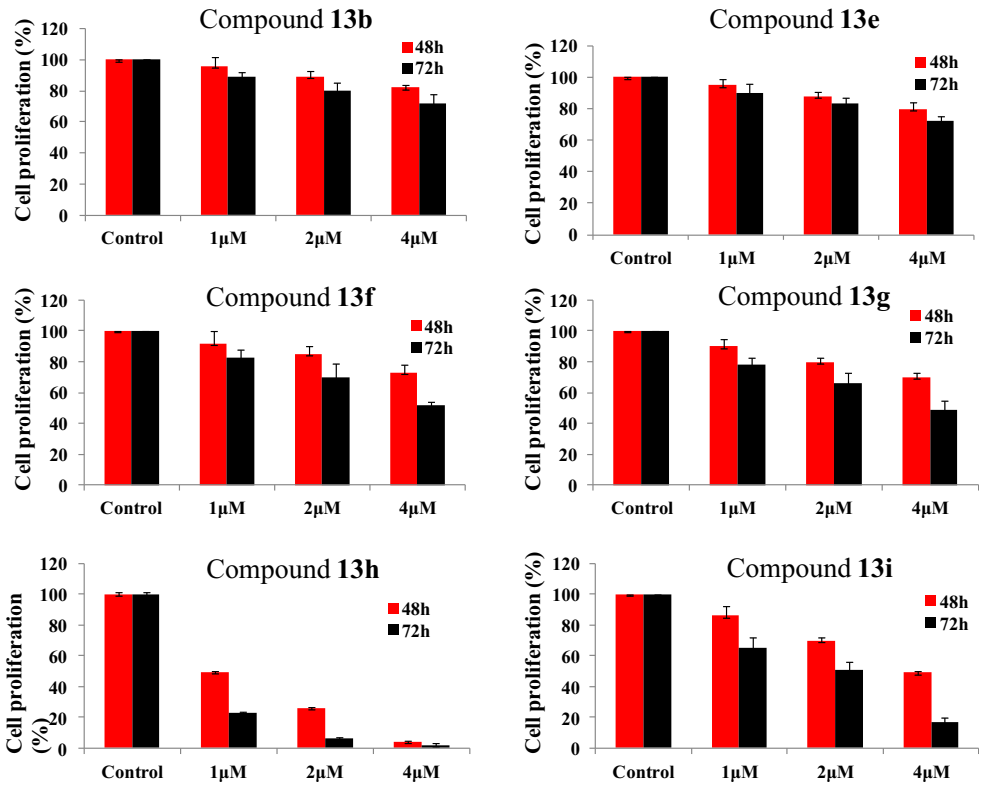

Fig. 4 Cell proliferation efficiency for phenothiazine hybrids against MGC-803 cells

13h could regulated the EMT process in a concentration-dependent manner.

Compound 10h inhibited tubulin polymerization

Recently, some papers have revealed that 1,2,3-triazole group was a promsing skeleton to design tubulin polymerization inhibitors [37, 38]. To confrm whether these designed 1,2,3-triazole-phenothiazine hybrids could bind to tubulin, phenothiazine hybrid **13h** was investigated for tubulin polymerization activity in vitro. As shown in Fig. 7, the fluorescence intensity was decreased in the presence of compound **13h** in a concentration-dependent manner. The IC_{50} value of tubulin polymerization activity was 2.87 μM. These results indicated that phenothiazine hybrid **13h** was a novel tubulin polymerization inhibitor.

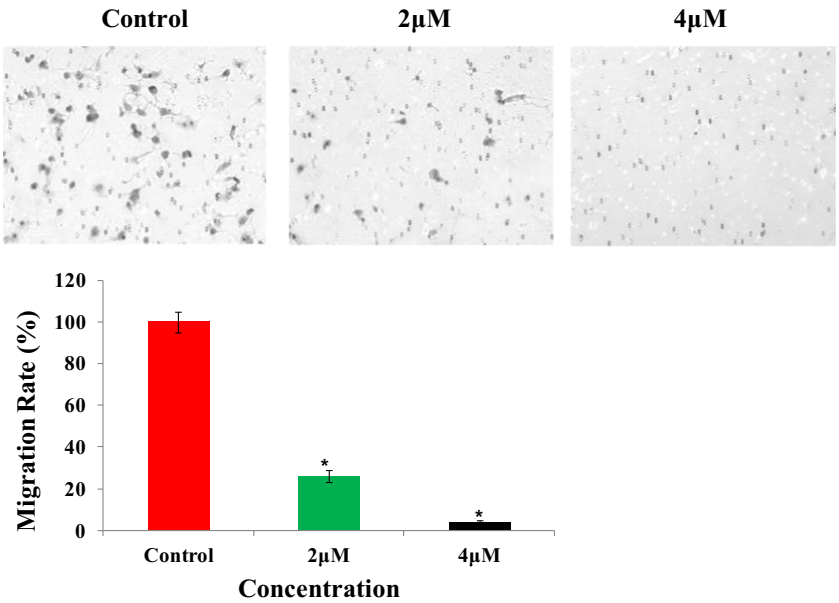

Fig. 5 The migration effect on MGC-803 cell line with compound **13h** treatment. *: $p < 0.05$ verse control

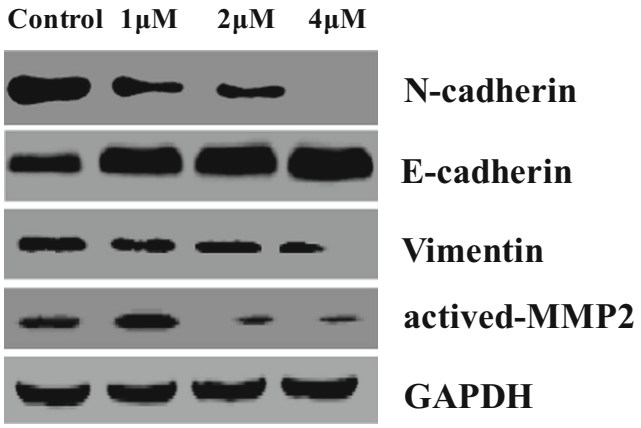

Fig. 6 Compound **13h** regulated the EMT related markers

Compound 10h regulated the Wnt/β-catenin signaling pathway

Wnt/β-catenin signaling pathway plays an important role in the regulation of embryonic development and tumorigenesis [39]. Since its deregulation results in severe human diseases, especially cancer, the wnt signaling pathway constitutes a promising platform for pharmacological targeting of cancer [40, 41]. In this work, we tested the expression level of wnt/β-catenin signaling pathway related markers (Wnt5α, β-catenin and TCF4). As shown in Fig. 8, phenothiazine hybrid **13h** decreased the expression level of Wnt5α, β-catenin and TCF4 in a concentration-dependent manner, suggesting that hybrid **13h** could regulate wnt/β-catenin signaling pathway.

Compound 10h inhibited tumor growth against a xenograft model

To further determine whether phenothiazine hybrid **13h** is a potential candidate drug for clinical application against gastric cancer, it was selected for in vivo testing against MGC-803 xenograft tumor growth in severe combined immunodeficiency (SCID) mice. From the antitumor results in Fig. 9, tumor volumes of drug treatment group were obviously decreased

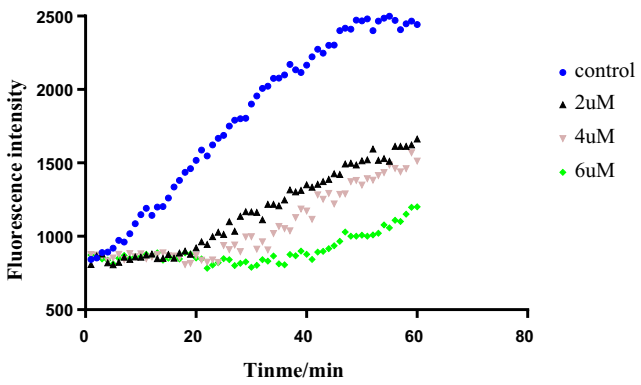

Fig. 7 Compound **13h** inhibited tubulin polymerization in vitro

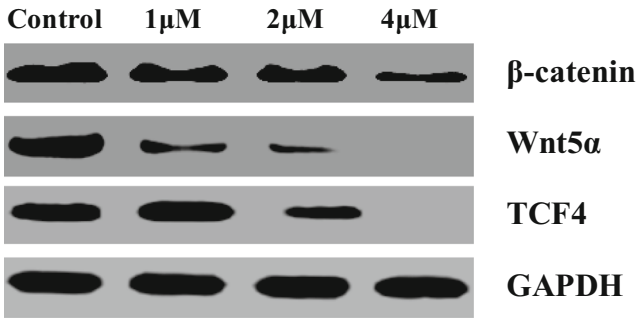

Fig. 8 Compound **13h** regulated the Wnt/β-catenin signaling pathway

compared with the normal group. The average tumor weights of control and 50 mg/kg drug treatment group were 1.440 ± 0.200 g, and 0.430 ± 0.250 g (inhibitory rate: 70.14%) respectively. Importantly, there was no apparent body weight loss in drug treatment group, indicating the low side effects of compound **13h** in vivo.

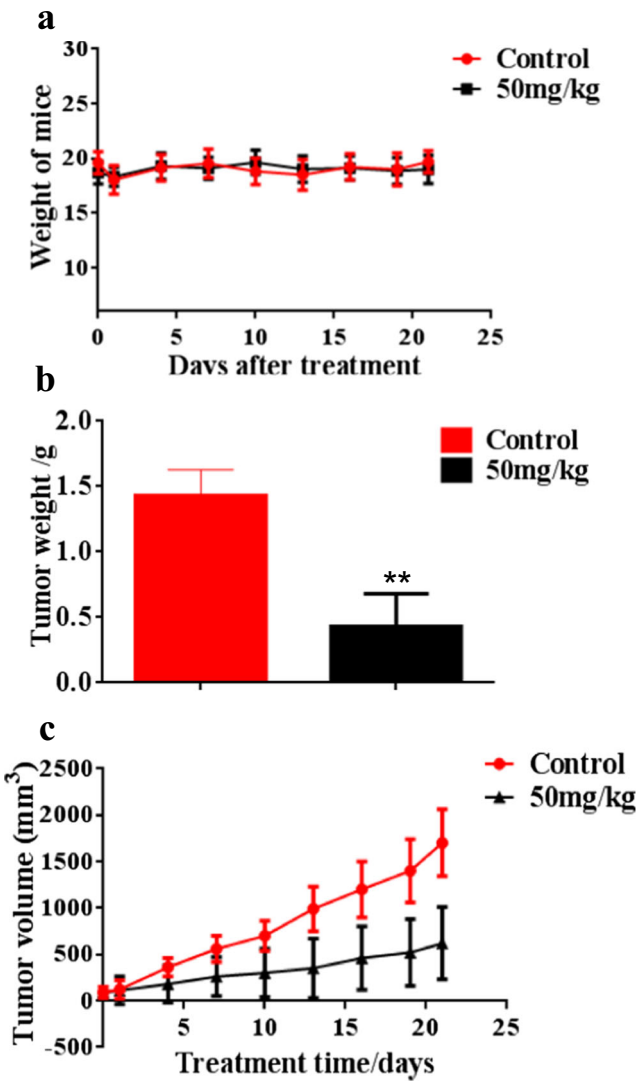

Fig. 9 1,2,3-triazole-phenothiazine hybrid 10h inhibited MGC-803 tumor growth in vivo. $^{**}P < 0.01$

Conclusions

In summary, novel phenothiazine hybrids were designed and synthesized by molecular hybridization strategy. Among them, compound **13h** displayed the most potent activity against MGC-803 cells with an IC_{50} value of 1.2 μM. Based on the mechanisms, we found that compound **13h** could inhibit MGC-803 cells migration by regulating wnt/β-catenin signaling pathway. Importantly, compound **13h** was revealed as a novel tubulin polymerization inhibitor and an orally active antitumor agent.

Acknowledgements This work was supported by the first affiliated hospital of zhengzhou university and First Affiliated Hospital of Henan University of Science and Technology.

Author contributions Nan Liu write the paper, do the synthetic work and biological research. Zhe Jin, Jing Zhang, and Jianjun Jin performed the synthetic work and biological research. All authors read and approved the final manuscript.

Funding This work was supported by the fund of First Affiliated Hospital of zhengzhou university and First Affiliated Hospital of Henan University of Science and Technology.

Compliance with ethical standards

Conflict of interest The authors declare that they have no conflict of interest.

Ethical approval This article does not contain any studies with human participants or animals performed by any of the authors.

Informed consent Informed consent was obtained from all individual participants included in the study.

References

1. Li L, Jiang S, Li X, Liu Y, Su J, Chen J (2018) Recent advances in trimethoxyphenyl (TMP) based tubulin inhibitors targeting the colchicine binding site. Eur J Med Chem 151:482–494
2. Xu L, Wang W, Meng T, Ma LP, Tong LJ, Shen JK, Wang YQ, Miao ZH (2018) New microtubulin inhibitor MT189 suppresses angiogenesis via the JNK-VEGF/VEGFR2 signaling axis. Cancer Lett 416:57–65
3. Herbst RS, Giaccone G, Schiller JH, Natale RB, Miller V, Manegold C, Scagliotti G, Rosell R, Oliff I, Reeves JA (2004) Gefitinib in combination with paclitaxel and carboplatin in advanced non–small-cell lung cancer: a phase III trial—INTACT 2. J Clin Oncol 22:785–794
4. Kreis W (2004) Docetaxel and estramustine compared with mitoxantrone and prednisone for advanced refractory prostate cancer. N Engl J Med 173:1513–1520
5. Wang Y, Yu Y, Li G-B, Li S-A, Wu C, Gigant B, Qin W, Chen H, Wu Y, Chen Q, Yang J (2017) Mechanism of microtubule stabilization by taccalonolide AJ. Nat Commun 8:15787
6. Pluta K, Morak-Młodawska B, Jeleń M (2011) Recent progress in biological activities of synthesized phenothiazines. Eur J Med Chem 46:3179–3189
7. Ghinet A, Moise I-M, Rigo B, Homerin G, Farce A, Dubois J (2016) Bîcu E, studies on phenothiazines: new microtubule-interacting compounds with phenothiazine A-ring as potent antineoplastic agents. Bioorg Med Chem 24:2307–2317
8. Brem B, Gal E, Găină L, Silaghidumitrescu L, Fischerfodor E, Tomuleasa CI, Grozav A, Zaharia V, Filip L, Cristea C (2017) Novel Thiazolo[5,4-b]phenothiazine derivatives: synthesis, structural characterization, and in vitro evaluation of antiproliferative activity against human leukaemia. Int J Mol Sci 18:1365
9. Ghorab MM, Alsaid MS, Samir N, Abdel-Latif GA, Soliman AM, Ragab FA, Abou El Ella DA (2017) Aromatase inhibitors and apoptotic inducers: design, synthesis, anticancer activity and molecular modeling studies of novel phenothiazine derivatives carrying sulfonamide moiety as hybrid molecules. Eur J Med Chem 134:304–315
10. Viegas-Junior C, Danuello A, Da SBV, Barreiro EJ, Fraga CA (2007) Molecular hybridization: a useful tool in the design of new drug prototypes. Curr Med Chem 14:1829
11. Saikia B, Saikia PP, Goswami A, Barua NC, Saxena AK, Suri N (2011) Synthesis of a novel series of 1,2,3-triazole-containing artemisinin dimers with potent anticancer activity involving Huisgen 1,3-dipolar cycloaddition reaction. Synthesis 2011:3173–3179
12. Marciniec K, Latocha M, Kurczab R, Boryczka S (2017) Synthesis and anticancer activity evaluation of a quinoline-based 1,2,3-triazoles. Med Chem Res 26:2432–2442
13. Allam M, Bhavani AKD, Mudiraj A, Ranjan N, Thippana M, Babu PP (2018) Synthesis of pyrazolo[3,4-d]pyrimidin-4(5H)-ones tethered to 1,2,3-triazoles and their evaluation as potential anticancer agents. Eur J Med Chem 156:43–52
14. Ruddarraju RR, Murugulla AC, Kotla R, Tirumalasetty MCB, Wudayagiri R, Donthabakthuni S, Maroju R (2017) Design, synthesis, anticancer activity and docking studies of theophylline containing 1,2,3-triazoles with variant amide derivatives. Med Chem Commun 8:176–183
15. Laskar S, Sánchez-Sánchez L, Flores SM, López-Muñoz H, Escobar-Sánchez ML, López-Ortiz M, Hernández-Rodríguez M, Regla I (2018) Identification of (1S,4S)-2,5-diazabicyclo[2.2.1]heptane-dithiocarbamate-nitrostyrene hybrid as potent antiproliferative and apoptotic inducing agent against cervical cancer cell lines. Eur J Med Chem 146:621–635
16. Li RD, Wang HL, Li YB, Wang ZQ, Wang X, Wang YT, Ge ZM, Li RT (2015) Discovery and optimization of novel dual dithiocarbamates as potent anticancer agents. Eur J Med Chem 93:381–391
17. Cao SL, Wang Y, Zhu L, Liao J, Guo YW, Chen LL, Liu HQ, Xu X (2010) Synthesis and cytotoxic activity of N-((2-methyl-4(3H)-quinazolinon-6-yl)methyl)dithiocarbamates. Eur J Med Chem 45:3850–3857
18. El-Naggar M, Almahli H, Ibrahim H, Eldehna W, Abdel-Aziz H (2018) Pyridine-Ureas as potential anticancer agents: synthesis and in vitro biological evaluation. Molecules 23:1459
19. Micoine K, Fürstner A (2010) Concise total synthesis of the potent translation and cell migration inhibitor Lactimidomycin. J Am Chem Soc 132:14064–14066
20. Jeng JH, Lan WH, Hahn LJ, Hsieh CC, Kuo YP (1996) Inhibition of the migration, attachment, spreading, growth and collagen synthesis of human gingival fibroblasts by arecoline, a major areca alkaloid, in vitro. J Oral Pathol Med 25:371–375
21. Xu Q, Bao K, Sun M, Xu J, Wang Y, Tian H, Zuo D, Guan Q, Wu Y, Zhang W (2017) Design, synthesis and structure-activity relationship of 3,6-diaryl-7H-[1,2,4]triazolo[3,4-b][1,3,4]thiadiazines as novel tubulin inhibitors. Sci Rep 7:11997
22. Chen W, Guo N, Qi M, Dai H, Hong M, Guan L, Huan X, Song S, He J, Wang Y, Xi Y, Yang X, Shen Y, Su Y, Sun Y, Gao Y, Chen Y, Ding J, Tang Y, Ren G, Miao Z, Li J (2017) Discovery, mechanism and metabolism studies of 2,3-difluorophenyl-linker-containing

PARP1 inhibitors with enhanced in vivo efficacy for cancer therapy. Eur J Med Chem 138:514–531
23. Liu H, Lu J, Hua Y, Zhang P, Liang Z, Ruan L, Lian C, Shi H, Chen K, Tu Z (2015) Targeting heat-shock protein 90 with ganetespib for molecularly targeted therapy of gastric cancer. Cell Death Dis 6: 1595
24. Hu M, Li J, Q-Yao S (2008) In situ "click" assembly of small molecule matrix metalloprotease inhibitors containing zinc-chelating groups. Org Lett 10:5529–5531
25. Angell YL, Burgess K (2007) Peptidomimetics via copper-catalyzed azide-alkyne cycloadditions. Chem Soc Rev 36:674–1689
26. Hou D, Che Z, Chen P, Zhang W, Chu Y, Yang D, Liu J (2018) Suppression of AURKA alleviates p27 inhibition on Bax cleavage and induces more intensive apoptosis in gastric cancer. Cell Death Dis 9:781
27. Nakatani Y, Kawakami H, Ichikawa M, Yamamoto S, Otsuka Y, Mashiko A, Takashima Y, Ito A, Nakagawa K, Arima S (2018) Nivolumab-induced acute granulomatous tubulointerstitial nephritis in a patient with gastric cancer. Invest New Drug 36:726–731
28. Tomasello G, Ghidini M, Liguigli W, Ratti M, Toppo L, Passalacqua R (2016) Targeted therapies in gastric cancer treatment: where we are and where we are going. Invest New Drug 34:378–393
29. Yoo C, Ryu MH, Na YS, Ryoo BY, Lee CW, Maeng J, Kim SY, Koo DH, Park I, Kang YK (2014) Phase I and pharmacodynamic study of vorinostat combined with capecitabine and cisplatin as first-line chemotherapy in advanced gastric cancer. Invest New Drug 32:271–278
30. Funakoshi Y, Mukohara T, Tomioka H, Ekyalongo RC, Kataoka Y, Inui Y, Kawamori Y, Toyoda M, Kiyota N, Fujiwara Y, Minami H (2013) Excessive MET signaling causes acquired resistance and addiction to MET inhibitors in the MKN45 gastric cancer cell line. Invest New Drug 31:1158–1168
31. Bonandi E, Christodoulou MS, Fumagalli G, Perdicchia D, Rastelli G, Passarella D (2017) The 1,2,3-triazole ring as a bioisostere in medicinal chemistry. Drug Discov Today 22:1572–1581
32. Abd-Rabou AA, Abdel-Wahab BF, Bekheit MS (2018) Synthesis, molecular docking, and evaluation of novel bivalent pyrazolinyl-1, 2,3-triazoles as potential VEGFR TK inhibitors and anti-cancer agents. Chem Pap 72:2225–2237
33. Miyakoshi H, Miyahara S, Yokogawa T, Endoh K, Muto T, Yano W, Wakasa T, Ueno H, Chong KT, Taguchi J, Nomura M, Takao Y, Fujioka A, Hashimoto A, Itou K, Yamamura K, Shuto S, Nagasawa H, Fukuoka M (2012) 1,2,3-Triazole-containing uracil derivatives with excellent pharmacokinetics as a novel class of potent human deoxyuridine triphosphatase inhibitors. J Med Chem 55:6427–6437
34. Chan SW, Lim CJ, Guo K, Ng CP, Lee I, Hunziker W, Zeng Q, Hong W (2008) A role for TAZ in migration, invasion, and tumorigenesis of breast cancer cells. Cancer Res 68:592–598
35. Aktas B, Tewes M, Fehm T, Hauch S, Kimmig R, Kasimirbauer S (2009) Stem cell and epithelial-mesenchymal transition markers on circulating tumor cells in patients with metastatic breast cancer. Cancer Res 69:107
36. Hazan RB, Phillips GR, Fang QR, Larry N, Aaronson SA (2000) Exogenous expression of N-cadherin in breast cancer cells induces cell migration, invasion, and metastasis. J Cell Biol 148:779–790
37. Solum EJ, Vik A, Hansen TV (2014) Synthesis, cytotoxic effects and tubulin polymerization inhibition of 1,4-disubstituted 1,2,3-triazole analogs of 2-methoxyestradiol. Steroids 87:46–53
38. Kamal A, Shaik B, Nayak VL, Nagaraju B, Kapure JS, Shaheer M-M, Shaik TB, Prasad B (2014) Synthesis and biological evaluation of 1,2,3-triazole linked aminocombretastatin conjugates as mitochondrial mediated apoptosis inducers. Bioorg Med Chem 22: 5155–5167
39. Chen D, Zhang H, Jing C, He X, Yang B, Cai J, Zhou Y, Song X, Li L, Hao X (2018) Efficient synthesis of new phenanthridine Wnt/β-catenin signaling pathway agonists. Eur J Med Chem 157:1491–1499
40. Ma H, Chen Q, Zhu F, Zheng J, Li J, Zhang H, Chen S, Xing H, Luo L, Zheng LT, He S, Zhang X (2018) Discovery and characterization of a potent Wnt and hedgehog signaling pathways dual inhibitor. Eur J Med Chem 149:110–121
41. Leow P-C, Bahety P, Boon CP, Lee CY, Tan KL, Yang T, Ee P-LR (2014) Functionalized curcumin analogs as potent modulators of the Wnt/β-catenin signaling pathway. Eur J Med Chem 71:67–80